Phonon anomalies and magnetic excitations in $BaFe_2Se_2O$

Feng Jin,[1] Nenad Lazarević,[2] Changle Liu,[3] Jianting Ji,[4] Yimeng Wang,[1] Shuna He,[1] Hechang Lei,[1] Cedomir Petrovic,[5] Rong Yu,[1] Zoran V. Popović,[2,6] and Qingming Zhang[4,7,*]

[1]*Department of Physics and Beijing Key Laboratory of Opto-electronic Functional Materials & Micro-nano Devices, Renmin University of China, Beijing 100872, China*

[2]*Center for Solid State Physics and New Materials, Institute of Physics Belgrade, University of Belgrade, Pregrevica 118, 11080 Belgrade, Serbia*

[3]*State Key Laboratory of Surface Physics and Department of Physics, Fudan University, Shanghai 200433, China*

[4]*Beijing National Laboratory for Condensed Matter Physics, Institute of Physics, Chinese Academy of Sciences, Beijing 100190, China*

[5]*Condensed Matter Physics and Materials Science Department, Brookhaven National Laboratory, Upton, New York 11973-5000, USA*

[6]*Serbian Academy of Sciences and Arts, Knez Mihailova 35, Belgrade 11000, Serbia*

[7]*School of Physical Science and Technology, Lanzhou University, Lanzhou 730000, China*

(Received 6 March 2019; revised manuscript received 4 April 2019; published 22 April 2019)

We report a temperature- and magnetic-field-dependent Raman-scattering study of the spin-ladder compound $BaFe_2Se_2O$. Temperature evolution of the B_{1g} mode self-energies revealed anomalous behavior at about 100 and 240 K with strong temperature-dependent Fano asymmetry. Furthermore, the A_g modes integrated intensity exhibits an additional change in tendency at about 50 K. All the observed anomalies can be traced back to spin-phonon interaction contributions as well as multiple magnetic phase transitions present in $BaFe_2Se_2O$ also detected in the Raman continuum induced by the spin fluctuations. Moreover, the absence of magnetic-field dependence of the magnetic mode observed at 436 cm^{-1} and the small linewidth and high intensity are different from the magnetic modes at about 650 cm^{-1}. This suggests a two-magnon continuum and a two-magnon bound state resonance for this mode.

DOI: 10.1103/PhysRevB.99.144419

I. INTRODUCTION

Quantum spin ladders have attracted much interest because of their fascinating properties and their possible relevance to the phase diagram of high-temperature superconducting cuprates [1–4]. The ground-state properties and the quasiparticle spectrum of the two-leg spin ladder have been studied theoretically [5–9] and experimentally [10–14]. Generally these systems may host various competing magnetic phases that are in close proximity.

Raman scattering offers a unique and powerful tool for probing lattice, spin, and charge excitations as well as interplay between them [4]. In the undoped spin ladder compound $La_6Ca_8Cu_{24}O_{41}$, the ladders contribute to a very broad two-triplet Raman line shape whose position is slightly different for leg-leg and rung-rung polarizations [15] in accordance with theoretical models [16]. However, in the spin-ladder and charge-ordered compound $Sr_{14}Cu_{24}O_{41}$, only a particularly sharp peak is observed at the same frequency for both polarizations [12,15]. Here, the spin-ladder (antiferromagnetic dimer) structure magnon related modes appear in the form of singularities of one-dimensional density of two-magnon states [11].

The iron-based compound $BaFe_2Se_2O$ is an experimental realization of a two-leg ladder structure [17–19]. In this compound, all iron ions are in the Fe^{2+} oxidation state with a high spin $S = 2$. The Fe_2Se_2O planes containing weakly coupled ladders are stacked along the c crystallographic axis. The ladder legs and rungs are along the b and a crystallographic axis, respectively. The basic magnetic properties of $BaFe_2Se_2O$ have been characterized by magnetic susceptibility and specific-heat measurements [17,18]. The magnetic susceptibility shows a broad maximum at $T_{max} \approx 450$ K and three successive magnetic phase transitions at $T \approx 240$, 115, and 43 K with T_{max} explained as due to the short-range correlation of the local moments [17] and the three magnetic phase transitions explained as either due to the antiferromagnetic phase transition (240 K) or due to the formation of spin-singlet dimers (115 and 43 K) [18]. Surprisingly, the specific-heat measurements indicate that the magnetic entropy up to 300 K is much smaller than the expected value. Local-spin-density-approximation calculations [17] suggest that the interaction along the rungs J is more than three times stronger than the interladder interaction J', whereas the interaction along the legs J'' can be neglected. A lattice dynamics study of $BaFe_2Se_2O$ was recently reported by Popović *et al.* [19]. They also observed a magnetic excitation related structure in the form of a magnon continuum with peaks corresponding to the singularities in the one-dimensional density of magnon states. In order to clarify the unusually large intensity of the lower-energy (magnon) peak and the origin of the B_{1g} modes line-shape asymmetry, a systematic Raman study, particularly in magnetic fields, is highly required.

In this paper, we report temperature- and field-dependent Raman-scattering measurements on $BaFe_2Se_2O$. The

*Corresponding author: qmzhang@ruc.edu.cn

temperature-dependent Raman spectra indicate the absence of a structural phase transition between 10 and 300 K, consistent with a moderate spin-phonon coupling. The Raman continuum observed only in the parallel polarization suggests strong spin fluctuations, and allows us to identify magnetic phase transitions at about 50, 100, and 240 K. The intensity of the sharp magnetic mode at 436 cm^{-1} exhibits a strong nonmonotonic field-dependent behavior with no observable energy shift with external magnetic fields up to 9 T. It is interpreted in terms of the two-magnon continuum and a two-magnon bound state resonance. The present study provides the fundamental lattice and spin dynamics information on $BaFe_2Se_2O$ and deepens the understanding of magnetic excitations in low-dimensional spin systems.

II. EXPERIMENTS

The $BaFe_2Se_2O$ single crystals used in this study were grown using the self-flux method. The details of crystal growth can be found elsewhere [18]. The average stoichiometry was checked using energy-dispersive x-ray spectroscopy (EDS; Oxford X-Max 50). The average atomic ratios determined from EDS are Ba:Fe:Se =1.0:1.9(2):2.0(2), close to the ratio of stoichiometric $BaFe_2Se_2O$. The presence of oxygen was confirmed for $BaFe_2Se_2O$, but the exact amount could not be quantified because of experimental limitations.

Freshly cleaved samples of (001) orientation were transferred into a UHV cryostat with a vacuum of better than 10^{-8} mbar. Temperature-dependent Raman spectra were collected with a Jobin Yvon LabRam HR800 spectrometer equipped with a volume Bragg grating low-wave-number suite, a liquid-nitrogen-cooled back-illuminated charge-coupled device detector, and a 633-nm laser (Melles Griot) with $\Gamma_\sigma < 0.1\ cm^{-1}$. The laser was focused into a spot of $\sim 5\ \mu m$ in diameter on the sample surface, with a power $< 100\ \mu W$, to avoid overheating. Magnetic-field-dependent Raman spectra were collected with a Jobin Yvon T64000 spectrometer also equipped with a liquid-nitrogen-cooled back-illuminated CCD. A 532-nm diode-pumped solid-state laser (Torus 532; Laser Quantum) was used as an excitation source. The laser was focused onto the samples with a spot size of 5–10 μm in diameter. The laser power was maintained at a level of 300 μW and monitored with a power meter (Coherent Inc.). Magnetic fields were generated up to 9 T using a superconducting magnet (Cryomagnetics) that has a room-temperature bore that is suitable for a microscope lens. The magnetic-field direction was perpendicular to the (001) plane of the sample.

In this paper, the Porto notation $i(jk)l$ is used for the scattering geometry, where i and l denote the direction and j and k the polarization of the incident and scattered light, respectively, and u stands for unpolarized light.

III. RESULTS AND DISCUSSION

A. Lattice dynamics and spin-phonon coupling

$BaFe_2Se_2O$ crystallizes in the orthorhombic crystal structure, described with space group $Pmmm$, with Ba and O atoms having C_{2v} site symmetry, whereas Fe and Se atoms have C_s site symmetry [19]. The symmetry analysis yields a total of 18 Raman-active modes $\Gamma_{\text{Raman}} = 6A_g + 2B_{1g} + 6B_{2g} + 4B_{3g}$, out of which, according to the Raman tensors below and the selection rules, only eight ($6A_g + 2B_{1g}$) are observable for our scattering geometry.

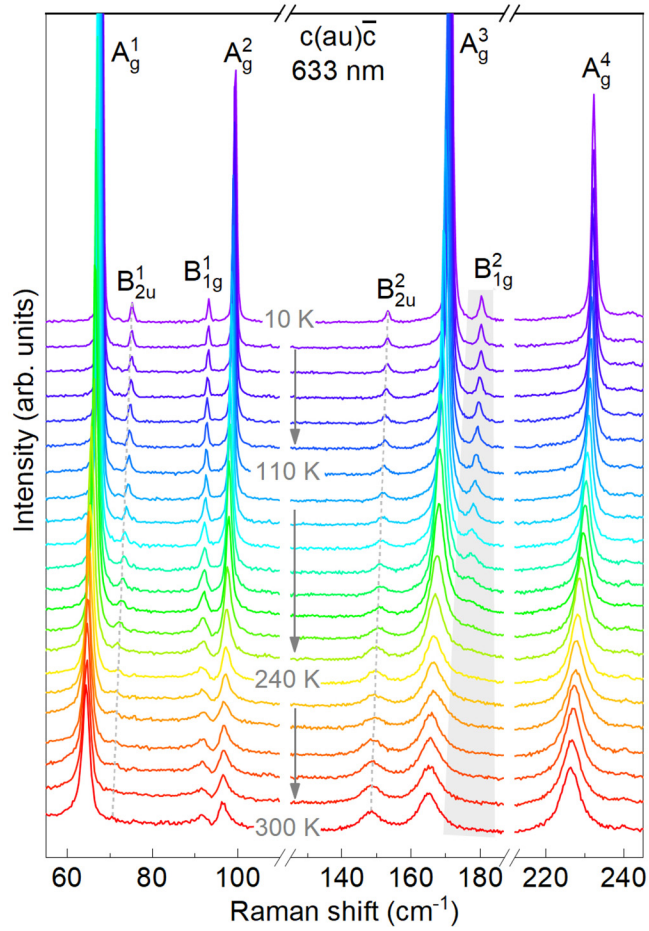

FIG. 1. Identification and temperature dependence of phonon modes in $BaFe_2Se_2O$. No change of crystal structure fingerprint was observed in the phonon spectra down to 10 K.

$$A_g = \begin{pmatrix} a & 0 & 0 \\ 0 & b & 0 \\ 0 & 0 & c \end{pmatrix}, \quad B_{1g} = \begin{pmatrix} 0 & d & 0 \\ d & 0 & 0 \\ 0 & 0 & 0 \end{pmatrix},$$

$$B_{2g} = \begin{pmatrix} 0 & 0 & e \\ 0 & 0 & 0 \\ e & 0 & 0 \end{pmatrix}, \quad B_{3g} = \begin{pmatrix} 0 & 0 & 0 \\ 0 & 0 & f \\ 0 & f & 0 \end{pmatrix}.$$

Figure 1 shows the temperature evolution of the $BaFe_2Se_2O$ Raman spectra in the temperature range between 10 and 300 K, in which eight phonon modes are observed. According to the lattice dynamical calculations [19], four A_g and two B_{1g} modes can be well assigned, as shown in Fig. 1. In addition to the A_g and B_{1g} symmetry modes, two peaks at about 75.2 and 153.3 cm^{-1} were also observed, which we previously attributed to new phonon modes due to the possible change of crystal symmetry accompanying the magnetic phase transition at $T_N = 240$ K [19]. As can be seen in Fig. 1, these peaks are also observable in our data even above T_N, indicating different origin. Energies are consistent with B_{2u}^1 and B_{2u}^2 infrared-active phonon modes, theoretically

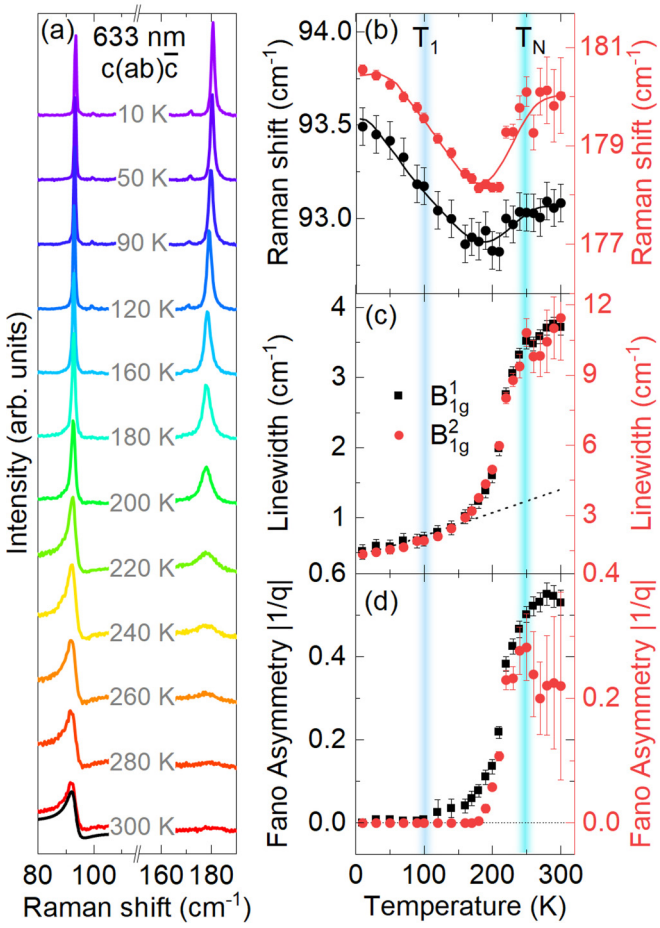

FIG. 2. Anomalies of B_{1g} modes induced by spin-lattice coupling. (a) Temperature dependence of Raman spectra for the $c(ab)\bar{c}$ polarization configuration, in which only the B_{1g} modes can be observed. The solid black line is a fit to a Fano line shape. Temperature dependence of the (b) frequency shift, (c) linewidth, and (d) Fano asymmetry parameters $|1/q|$ of B^1_{1g} (left axis, black) and B^2_{1g} (right axis, red) modes. The solid lines in (b) represent a fit to Eq. (1) and the dotted line in (c) represents the behavior expected from anharmonicity.

predicted by density functional theory calculations [19], and we assign them accordingly. Their observability in Raman data may stem from the release of symmetry selection rule by the structural imperfections. In our previous paper [18], Mössbauer data suggested oxygen deficiency, i.e., O_{1-x} composition for $BaFe_2Se_2O$. This might be the source of structural imperfections.

First, we focus on B_{1g} phonon modes, which display a pronounced asymmetry at high temperatures ($T > T_N$) that is suppressed at low temperatures ($T \ll T_N$), as can be seen in Fig. 2(a). Having in mind small instrumental broadening, the analysis of the line shape was preformed by using Fano function alone [20,21]: $I(\omega) = I_0(q+\varepsilon)^2/(1+\varepsilon^2)$, where $\varepsilon = (\omega - \omega_0)/\Gamma$, ω_0 is the bare phonon frequency, Γ is the linewidth, and q is the asymmetry parameter [22]. Frequency shift, linewidth, and Fano asymmetry parameter $|1/q|$ for both modes as a function of temperature are presented in Figs. 2(b), 2(c), and 2(d), respectively. Whereas they exhibit very similar temperature dependence, upon heating from 10 K a small deviation from the "standard" anharmonic type of behavior can be noticed at about $T_1 = 100$ K accompanied by the appearance of the line-shape asymmetry. Further heating results in a significant renormalization of the phonon self-energies around T_N with the Fano asymmetry parameters reaching maximum value in the same temperature region.

The pronounced Fano asymmetry observed for the B_{1g} modes above T_N [Fig. 2(d)] indicates strong coupling to a continuum of excitations. Here we attribute the continuum to the magnetic scattering stemming from the spin fluctuation, which will be further discussed below. In comparison, an electronic mechanism for the continuum is unlikely as $BaFe_2Se_2O$ is electrically insulating with a transport gap of 1.86 eV [17]. According to the lattice dynamical calculations [19], the B_{1g} modes are mainly due to the vibration of Fe and Se atoms along the b axis which mediate the magnetic interaction. Therefore, one could expect B_{1g} modes to couple to the magnetic scattering.

The coupling of B_{1g} modes to the spin system is also reflected in the abnormal behaviors of their linewidth. To demonstrate this, we have included in Fig. 2(c) plots of the behavior expected from anharmonicity, $\Gamma(T) = \Gamma_0[1 + 2/(e^{\hbar\omega/2k_BT} - 1)]$. The fit strongly deviates already around 170 K, implying an additional relaxation mechanism which we ascribe to spin-phonon coupling. Such coupling is very pronounced in low-dimensional spin dimer systems, as well as in two- and three-dimensional frustrated spin systems [23–25].

In order to estimate the spin-phonon coupling constant in $BaFe_2Se_2O$, we may approximate phonon frequency temperature dependence as

$$\omega(T) = \omega(0) - C\left(1 + \frac{2}{e^x - 1}\right) + \lambda\langle S_iS_j\rangle, \qquad (1)$$

where $\omega(0)$ is the harmonic frequency of an optical mode at zero temperature, $x = \hbar\omega(0)/2k_BT$, λ is the spin-phonon coupling constant, $\langle S_iS_j\rangle$ represents the spin-spin correlation function, and C is an anharmonic constant. The second term in Eq. (1) describes the anharmonic phonon contribution based on symmetrical optical phonon decay into acoustic phonons [26], whereas the third term represents the contribution from the spin-phonon coupling based on the Baltensperger and Helman model [27,28]. If we take into account only the nearest-neighbor interactions, the spin-spin correlation function $\langle S_iS_j\rangle_\chi$ can be written as [25]

$$\langle S_iS_j\rangle_\chi = \frac{k_BT\chi_m(T)}{N_Ag^2\mu_B^2} - \frac{S(S+1)}{3}, \qquad (2)$$

where $g = 2$, $S = 2$, and the magnetic susceptibility $\chi_m(T)$ is given in Ref. [18]. We can now analyze the B_{1g} symmetry modes frequency temperature dependance within Eq. (1) [see solid lines in Fig. 2(b)]. This yields the spin-phonon coupling constants $\lambda(B^1_{1g}) = 1.8$ cm^{-1}, $\lambda(B^2_{1g}) = 12.8$ cm^{-1}, and the anharmonic constant $C(B^1_{1g}) = 0.33$ cm^{-1}, $C(B^2_{1g}) = 4.76$ cm^{-1}. The individual contribution due to anharmonic and spin-phonon coupling can be found in Fig. 5 in Appendix A. Obtained spin-phonon coupling constants are smaller than those in the spin-Peierls system $CuGeO_3$, where spin-phonon

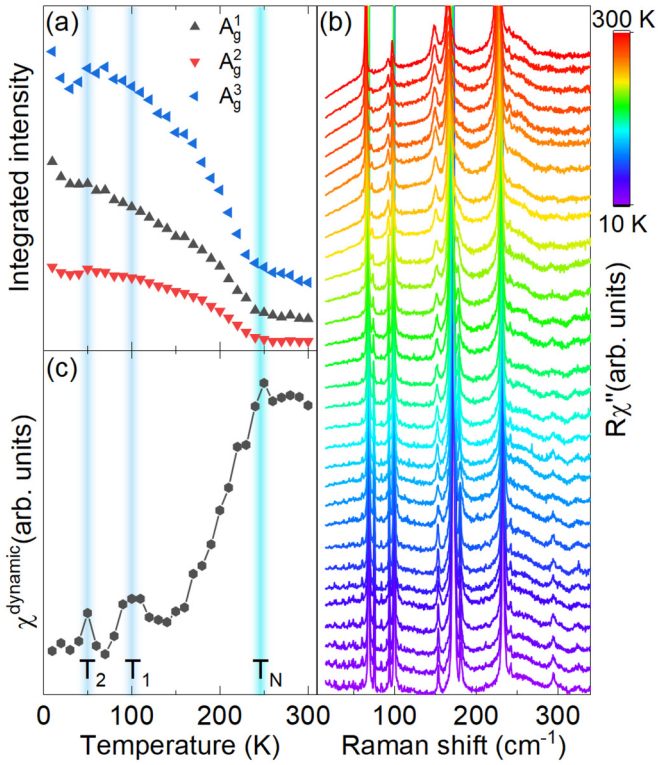

FIG. 3. (a) Integrated intensity of the A_g^1, A_g^2, and A_g^3 symmetry modes as a function of temperature. (b) Temperature evolution of Raman susceptibility data for $BaFe_2Se_2O$ obtained in parallel scattering configuration. The pronounced Raman continuum evolution is observable only in parallel [i.e., (*aa*) or (*bb*)] and absent in cross polarization configurations [i.e., (*ab*) or (*ba*)] (not shown). (c) Temperature dependence of dynamical susceptibility $\chi^{\text{dynamic}}(T)$ obtained from the Raman data.

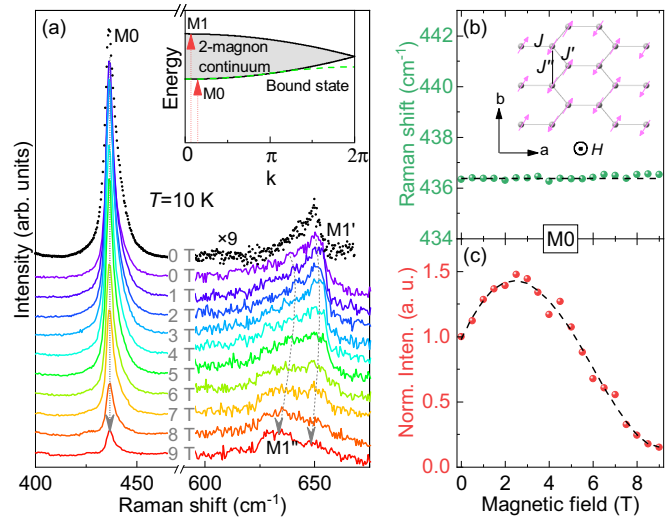

FIG. 4. Identification of magnetic excitations in $BaFe_2Se_2O$. (a) Field-dependent Raman spectra, measured at 10 K with 532-nm laser line (solid lines). The spectrum (dotted line) collected at 0 T with a 633-nm laser are also shown for comparison. Inset: Schematic spin excitation spectrum of $BaFe_2Se_2O$. The green dashed line represents a possible two-magnon bound state. Field dependence of the (b) energy and (c) intensity of the $M0$ mode. Inset of (b): Schematic representation of the periodic magnetic structure in the (*ab*) plane. J represents Fe-O-Fe antiferromagnetic (AFM) exchange interaction along the rungs; J' is the interladder Fe-Se-Fe AFM exchange interaction. J'' is the ferromagnetic Fe-Se-Fe exchange interaction along the ladder legs and can be neglected.

coupling constants of $\lambda_{103} = -10$ cm^{-1}, $\lambda_{215} = 40$ cm^{-1}, $\lambda_{366} = -21$ cm^{-1}, and $\lambda_{812} = -8$ cm^{-1} were found [29]. Thus moderate spin-phonon coupling constants in $BaFe_2Se_2O$ may account for the absence of a structural phase transition at the magnetic phase transition.

Now we turn our attention to the A_g symmetry modes. As can be seen from Fig. 3(a), the integrated intensity temperature dependence of the analyzed A_g modes exhibits clear discontinuity at T_N. In addition, another change in tendency has been observed at about $T_2 = 50$ K.

Whereas the phonon anomalies at T_N can be directly traced back to the spin dynamics, the origin of the phonon anomalies at T_1 and T_2 is not clear. To clarify this, we analyze the Raman continuum that nonmonotonically develops in the A_{1g} channel with temperature [see Fig. 3(a)], as expected for the (quasi-) one-dimensional spin systems [30–32]. Directly from the Raman data, dynamic Raman susceptibility [33] can be calculated using the Kramers-Kronig relation $\chi^{\text{dynamic}} = \lim_{\omega\to 0}\chi(q=0,\omega) \propto \int_0^\infty \frac{\chi''}{\omega} d\omega$. Since we do not attempt to quantitatively analyze the spin-fluctuation contributions, which falls beyond the scope of our work, but to pinpoint possible magnetic phase transition, we approximate $\chi^{\text{dynamic}}(T)$ as an integral of the Raman conductivity data after excluding the contributions from phonons. As can be seen in Fig. 3(c), $\chi^{\text{dynamic}}(T)$ strongly increases upon approaching T_N after which it saturates in the paramagnetic phase where the spins are not correlated. At low temperatures it develops two peak-like features coinciding with observed anomalies in the lattice dynamic thus indicating their spin dynamics related origin. Furthermore, $\chi^{\text{dynamic}}(T)$ exhibits good agreement with the previously reported magnetic susceptibility data [18], indicating additional magnetic phase transitions in $BaFe_2Se_2O$ at low temperatures.

B. Two-magnon Raman scattering

The two asymmetric peaks at 436 and 653 cm^{-1} (see Fig. 4) have been reported before and assigned as a magnetic excitation related structure due to their special polarization and temperature-dependent characterizations [19]. However, the extremely high intensity of the 436 cm^{-1} ($M0$) mode suggests an additional mechanism that comes into play, other than those manifested with the 653 cm^{-1} mode. In particular, compared with the linewidth of two-magnon modes in other two-dimensional (2D) spin systems, the $M0$ linewidth of only $\sim$5 cm^{-1} at 15 K is quite unusual for a 2D spin-ladder system. For example, the linewidth of the two-magnon mode is $\sim$800 cm^{-1} for $Sr_2Cu_2O_2Cl_2$ [34], whereas it is $\sim$500 cm^{-1} in $La_6Ca_8Cu_{24}O_{41}$ [13]. To the best of our knowledge, the sharpest two-magnon mode so far was found in CaV_2O_5 with a width of more than 50 cm^{-1} [10], still one order of magnitude larger than that in $BaFe_2Se_2O$.

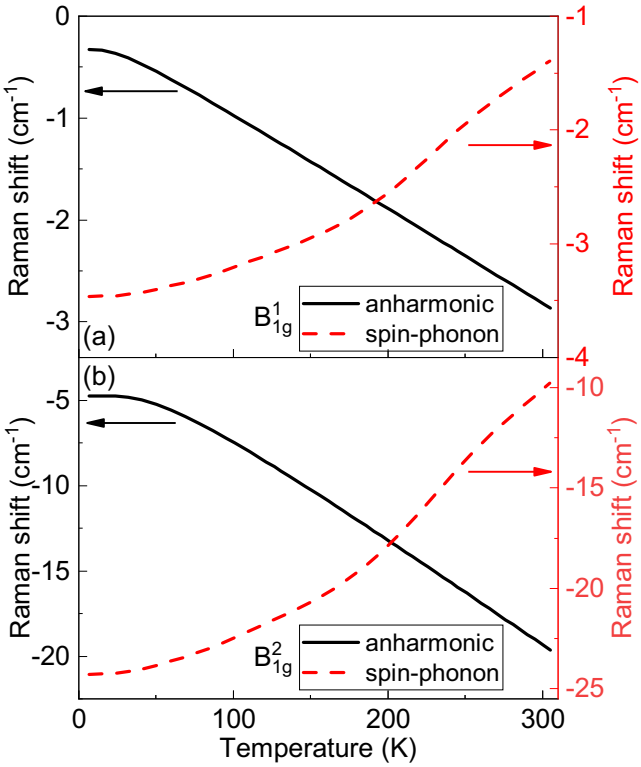

FIG. 5. Anharmonic (solid line) and spin-phonon (dashed line) contribution to the temperature dependence of the energy of (a) B^1_{1g} and (b) B^2_{1g} phonon modes obtained by fitting Eq. (1) to the experimental data.

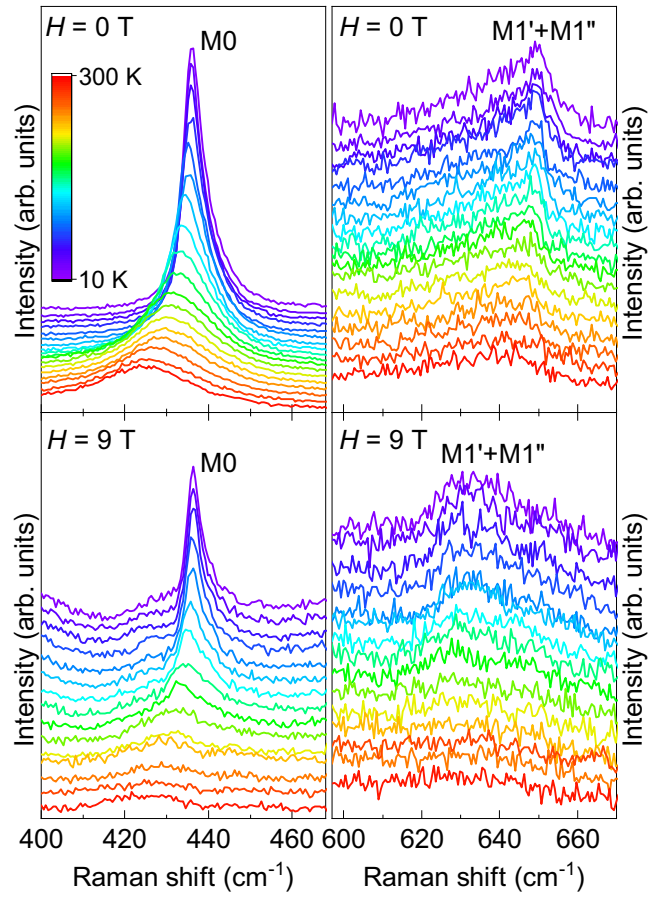

FIG. 6. Temperature-dependent spectra of the $M0$, $M1'$, and $M1''$ modes at 0 and 9 T.

To clarify the origin of the unusual $M0$ mode, the magnetic-field- and temperature-dependent Raman experiments have been performed on $BaFe_2Se_2O$ crystals [Fig. 4(a) and Fig. 6 in Appendix B]. The field dependence of the energy and intensity of the $M0$ mode are summarized in Figs. 4(b) and 4(c). It can be seen that both the $M0$ energy and the linewidth are nearly field independent, whereas the intensity exhibits a strong nonmonotonic field dependence. The intensity slightly increases with magnetic fields below 3 T, but quickly drops down above 3 T and almost vanishes for $B = 9$ T. A closer inspection of the 653-cm^{-1} peak magnetic-field-dependent spectra reveals its two-peak nature ($M1'$ and $M1''$; see Fig. 4). Both peaks harden up to 3 T after which they soften. Whereas the $M1'$ intensity follows the $M0$ mode behavior, $M1''$ experiences a constant gain of intensity. The strong field dependence of $M0$, $M1'$, and $M1''$ as well as their special polarization and temperature-dependent characterizations [19] confirms that these modes are indeed magnon related, but not due to some structural imperfections.

In general, several theoretical scenarios can be considered to account for the strength and sharpness of the magnon modes in the 2D system: (i) backfolding of the triplet dispersion due to charge ordering [13]; (ii) large anisotropy of the magnetic exchanges along rung and leg directions [35]; and (iii) the resonance between the two-magnon continuum and a two-magnon bound state [16,36]. In $BaFe_2Se_2O$, the origin of dispersion backfolding can be excluded because of its electrically insulating nature. Although the large anisotropy between J'' and J explains the observation of the $M0$ mode at the given energy, it alone cannot account for the intensity and its magnetic-field dependence. This kind of behavior can be observed in the presence of the resonance between the two-magnon continuum and a two-magnon bound state.

In low-dimensional antiferromagnets, a strong magnon-magnon interaction induces a magnetic bound state [31,37–40] that merges with the two-magnon continuum at zero momentum (schematically shown in Fig. 4). This allows a resonance at the bottom of the continuum and contributes to the asymmetric line shape [36]. Such a resonance can well explain the strength, sharpness, and asymmetry of the $M0$ mode. The field dependence of the $M0$ mode intensity provides further support for the picture. External magnetic fields usually lead to a spin canting or even a spin flop/flip transition [41] and consequently modulate the magnon excitation spectrum. In $BaFe_2Se_2O$, the modulation of the magnon excitation spectrum is evidenced by the energy shift of the $M1'$ and$M1''$ modes (Fig. 4). A quantitative understanding of the $M0$, $M1'$, and $M1''$ modes magnetic-field dependence requires more theoretical work in the future and goes beyond the scope of this paper.

IV. SUMMARY

In summary, a $BaFe_2Se_2O$ temperature- and field-dependent Raman-scattering study has been performed. The

temperature evolution of the Raman-active modes indicates that there is no structural phase transition accompanying the magnetic phase transitions. Observed anomalies in the phonon spectra can be traced back to moderate spin-phonon interaction contributions as well as multiple magnetic phase transitions present in $BaFe_2Se_2O$ also detected in the Raman continuum induced by the spin fluctuations. The anomalous intensity of the $M0$ peak is attributed to the contribution from the two-magnon continuum and a two-magnon bound state resonance. The present study provides the fundamental lattice and spin dynamics information on $BaFe_2Se_2O$ and is of significance for the understanding of magnetic excitations in low-dimensional spin systems.

ACKNOWLEDGMENTS

This work was supported by the National Natural Science Foundation of China, the Ministry of Science and Technology of China, the Fundamental Research Funds for the Central Universities, the Research Funds of Renmin University of China and Serbian Ministry of Education, Science and Technological Development under Project III45018. The work at Brookhaven National Laboratory was supported by the U.S. DOE under Contract No. DE-SC0012704 (material synthesis).

APPENDIX A: ANHARMONIC AND SPIN-PHONON CONTRIBUTIONS TO PHONON MODE ENERGIES

In this Appendix, we show the individual contribution of anharmonic and spin-phonon terms to the temperature dependence of the energy of the two B1g modes (Fig. 5), which are obtained by fitting Eq. (1) to the experimental data.

APPENDIX B: TEMPERATURE- AND FIELD-DEPENDENT RAMAN SPECTRA

To explore the origin of the magnetic scattering modes, we performed temperature-dependent Raman experiments and the collected spectra of the M0 M1' and M1" modes at 0 and 9 T are shown in Fig. 6. One can see that these modes exhibit distinctive temperature dependent behaviors, namely, a characteristic decrease in energy and intensity, and an increase in linewidth, with increasing temperature, reflecting the renormalization of magnon energies and lifetimes by thermally excited carriers.

[1] P. W. Anderson, Science **235**, 1196 (1987).
[2] E. Dagotto and T. M. Rice, Science **271**, 618 (1996).
[3] E. Dagotto, Rep. Prog. Phys. **62**, 1525 (1999).
[4] P. Lemmens, G. Güntherodt, and C. Gros, Phys. Rep. **375**, 1 (2003).
[5] T. Barnes, E. Dagotto, J. Riera, and E. S. Swanson, Phys. Rev. B **47**, 3196 (1993).
[6] T. Barnes and J. Riera, Phys. Rev. B **50**, 6817 (1994).
[7] S. R. White, R. M. Noack, and D. J. Scalapino, Phys. Rev. Lett. **73**, 886 (1994).
[8] S. Gopalan, T. M. Rice, and M. Sigrist, Phys. Rev. B **49**, 8901 (1994).
[9] D. G. Shelton, A. A. Nersesyan, and A. M. Tsvelik, Phys. Rev. B **53**, 8521 (1996).
[10] M. J. Konstantinović, Z. V. Popović, M. Isobe, and Y. Ueda, Phys. Rev. B **61**, 15185 (2000).
[11] Z. V. Popović, M. J. Konstantinović, V. A. Ivanov, O. P. Khuong, R. Gajić, A. Vietkin, and V. V. Moshchalkov, Phys. Rev. B **62**, 4963 (2000).
[12] A. Gozar, G. Blumberg, B. S. Dennis, B. S. Shastry, N. Motoyama, H. Eisaki, and S. Uchida, Phys. Rev. Lett. **87**, 197202 (2001).
[13] K. P. Schmidt, C. Knetter, M. Grüninger, and G. S. Uhrig, Phys. Rev. Lett. **90**, 167201 (2003).
[14] A. Gößling, U. Kuhlmann, C. Thomsen, A. Löffert, C. Gross, and W. Assmus, Phys. Rev. B **67**, 052403 (2003).
[15] S. Sugai and M. Suzuki, Phys. Status Solidi B **215**, 653 (1999).
[16] K. P. Schmidt, C. Knetter, and G. S. Uhrig, Europhys. Lett. **56**, 877 (2001).
[17] F. Han, X. Wan, B. Shen, and H.-H. Wen, Phys. Rev. B **86**, 014411 (2012).
[18] H. Lei, H. Ryu, V. Ivanovski, J. B. Warren, A. I. Frenkel, B. Cekic, W.-G. Yin, and C. Petrovic, Phys. Rev. B **86**, 195133 (2012).
[19] Z. V. Popović, M. Šćepanović, N. Lazarević, M. M. Radonjić, D. Tanasković, H. Lei, and C. Petrovic, Phys. Rev. B **89**, 014301 (2014).
[20] A. Baum, A. Milosavljević, N. Lazarević, M. M. Radonjić, B. Nikolić, M. Mitschek, Z. I. Maranloo, M. Šćepanović, M. Grujić-Brojčin, N. Stojilović, M. Opel, A. Wang, C. Petrovic, Z. V. Popović, and R. Hackl, Phys. Rev. B **97**, 054306 (2018).
[21] A. Milosavljević, A. Šolajić, J. Pešić, Y. Liu, C. Petrovic, N. Lazarević, and Z. V. Popović, Phys. Rev. B **98**, 104306 (2018).
[22] U. Fano, Phys. Rev. **124**, 1866 (1961).
[23] M. Braden, B. Hennion, W. Reichardt, G. Dhalenne, and A. Revcolevschi, Phys. Rev. Lett. **80**, 3634 (1998).
[24] K.-Y. Choi, Y. G. Pashkevich, K. V. Lamonova, H. Kageyama, Y. Ueda, and P. Lemmens, Phys. Rev. B **68**, 104418 (2003).
[25] C. Kant, J. Deisenhofer, T. Rudolf, F. Mayr, F. Schrettle, A. Loidl, V. Gnezdilov, D. Wulferding, P. Lemmens, and V. Tsurkan, Phys. Rev. B **80**, 214417 (2009).
[26] J. Menéndez and M. Cardona, Phys. Rev. B **29**, 2051 (1984).
[27] W. Baltensperger and J. S. Helman, Helv. Phys. Acta **41**, 668 (1968).
[28] W. Baltensperger, J. Appl. Phys. **41**, 1052 (1970).
[29] R. Werner, C. Gros, and M. Braden, Phys. Rev. B **59**, 14356 (1999).
[30] T. Sekine, M. Jouanne, C. Julien, and M. Balkanski, Phys. Rev. B **42**, 8382 (1990).
[31] P. Lemmens, M. Grove, M. Fischer, G. Güntherodt, V. N. Kotov, H. Kageyama, K. Onizuka, and Y. Ueda, Phys. Rev. Lett. **85**, 2605 (2000).

[32] K. Y. Choi, J. W. Hwang, P. Lemmens, D. Wulferding, G. J. Shu, and F. C. Chou, Phys. Rev. Lett. **110**, 117204 (2013).

[33] A. Glamazda, P. Lemmens, S. H. Do, Y. S. Choi, and K. Y. Choi, Nat. Commun. **7**, 12286 (2016).

[34] G. Blumberg, P. Abbamonte, M. V. Klein, W. C. Lee, D. M. Ginsberg, L. L. Miller, and A. Zibold, Phys. Rev. B **53**, R11930 (1996).

[35] K. P. Schmidt, A. Gössling, U. Kuhlmann, C. Thomsen, A. Löffert, C. Gross, and W. Assmus, Phys. Rev. B **72**, 094419 (2005).

[36] C. Jurecka, V. Grützun, A. Friedrich, and W. Brenig, Eur. Phys. J. B **21**, 469 (2001).

[37] O. P. Sushkov and V. N. Kotov, Phys. Rev. Lett. **81**, 1941 (1998).

[38] G. Bouzerar, A. P. Kampf, and G. I. Japaridze, Phys. Rev. B **58**, 3117 (1998).

[39] M. Windt, M. Grüninger, T. Nunner, C. Knetter, K. P. Schmidt, G. S. Uhrig, T. Kopp, A. Freimuth, U. Ammerahl, B. Büchner, and A. Revcolevschi, Phys. Rev. Lett. **87**, 127002 (2001).

[40] C. Knetter, K. P. Schmidt, M. Grüninger, and G. S. Uhrig, Phys. Rev. Lett. **87**, 167204 (2001).

[41] S. Blundell, in *Magnetism in Condensed Matter* (Oxford University Press, New York, 2001).